PCCP

Accepted Manuscript

ROYAL SOCIETY OF CHEMISTRY

www.rsc.org/pccp

Structural and dynamical anomalies of soft particles interacted with harmonic repulsions

Wenze Ouyang,*[a], Bin Sun[b], Zhiwei Sun[a], and Shenghua Xu‡[a]

Molecular dynamics(MD) simulations are carried out to investigate the structural and dynamical anomalies in the core-softened fluid with harmonic repulsions. At sufficiently low temperature and densities, a general scaling relation between Rosenfeld's diffusivity D_R and excess entropy S_{ex} hold true because the ultrasoft particles tend to avoid overlaps and behave like effective hard spheres. When the temperature is increased to high enough, the system acts as a weakly correlated mean-field fluid so that an alternative scaling relation between temperature scaled diffusion D_T and S_{ex} does work. Interestingly, the plots of D_R versus two-body excess entropy S_2 approximately collapse onto a single master curve despite the structural and dynamical anomalies, which has also been observed in other core-softened fluids with bounded potential.

0 [a] *Key Laboratory of Microgravity(National Microgravity Laboratory), Institute of Mechanics, Chinese Academy of Sciences, Beijing 100190, People's Republic of China. Fax: +86 1082544096; Tel: +86 1082544099; E-mail: oywz@imech.ac.cn*

0 [b] *School of Materials and Chemical Engineering, Zhongyuan University of Technology, Zhengzhou 450007, People's Republic of China.*

0 ‡ *Email: xush@imech.ac.c*

1 Introduction

It has been known that most liquids become denser upon cooling and more viscous upon compression. However, water and some other liquids with tetrahedrality such as silica, silicon, carbon, and phosphorus have been found to exhibit anomalous behavior close to their freezing lines[1], i.e, their phase diagrams have regions where thermal expansion coefficient is negative, self-diffusivity increases upon compression, and the structural order of the system decreases with increasing pressure. Jagla showed in the pioneering paper that these anomalies are originated from the existence of two different preferred interparticle separations[2]. Afterwards, a few more simple models with spherically symmetric potentials which can also generate anomalies have been proposed[3–10].

The interactions between particles of simple atomic and molecular liquids are generally steeply repulsive when the particles get more and more close to each other. But soft particles, such as macromolecules and their self-assembled entities, emulsions, soft colloids and grains etc, have softer effective pair interactions. As the shape of the pair potential often determines the phase behavior of the system[11], one can expect that the phase behavior of soft particles will have a wide differs from that of hard ones. Some types of soft particles may elastically deform and even mutually interpenetrate when colliding with each other, so their phase behaviors become more complex. Actually, it does not necessarily require a singular repulsion for vanishing interparticle separations in some systems with core-softened particles. In this respect, it is interesting to consider an extreme class of repulsive potentials that are bounded, i.e, they remain finite for the whole range of interparticle separations, even at full overlap between the particles[11,12]. Many previous studies have shown that the systems with bounded potential have rich and complex phase behaviors[4–7,13–24]. Among those phase behaviors, the anomalies of the systems with core-softened particles have attracted much interest in recent years[4–7,13–15].

To fully characterize the thermodynamic and dynamic behavior among the studies of liquids, the connection between the diffusion coefficient D and the excess entropy S_{ex} is of fundamental interest. It not only provides a clue in the long-standing puzzle concerning how the structural and thermodynamic properties correlate with the dynamics of fluids, but also has practical consequences. For instance, if the diffusion coefficient can be approximately represented as a single-valued function of the excess entropy, then knowledge of the latter allows indirect prediction of the former. In 1977, Rosenfeld first proposed that the reduced diffusion coefficient can be connected to the excess entropy of the system through the formula[25]

$$D_R = A \exp\left(BS_{ex}\right), \tag{1}$$

where A and B are the constants which interestingly show an extremely weak dependence on the material and can be considered universal. The excess entropy S_{ex}, which refers to the difference between the entropy per particle of the fluid and that of an ideal gas of particles with the same number density ρ, is a negative

quantity. The diffusion coefficient is expressed in reduced units based on the mean length related to the density of the system $\rho^{-1/3}$ and to the thermal velocity $(k_BT/m)^{1/2}$ so that $D_R = D\rho^{1/3}T^{-1/2}$. Afterwards, Rosenfeld further extended the quasi-universal excess-entropy scaling to the regime of dilute gas, where $-S_{ex}$ is low and the power-law form follows from Enskog theory for D[26]

$$D_R = \alpha(-S_{ex})^{\beta}\ , \tag{2}$$

where α and β are constants too. Although the original idea is to associate the system under investigation to the hard-sphere system, it has been demonstrated that the entropy scaling relations developed by Rosenfeld are valid in various model fluids[26–28]. Here one may ask the question whether the Rosenfeld scaling relations are still valid in the fluids with ultrasoft particles which are essentially different from the hard spheres. Krekelberg et al studied the anomalous behaviors of Gaussian-core(GC) fluid, which belongs to a class of bounded potentials, showing that the Rosenfeld diffusivity D_R is approximately a function of two-body excess entropy S_2 alone and that a different combination $D_T = DT^{-1/2}$ collapses as a function of S_{ex}[4]. Fomin and coworkers observed that the Rosenfeld scaling formula for the fluids of GC and Hertzian spheres is valid only in the infinite-temperature limit where there are no anomalies[6]. Until now, whether these observations will generally hold for other fluids with bounded potential is still an open issue and it needs more detailed study.

In this paper, we give a further study on the anomalous behaviors of another type of core-softened fluid with bounded potential. The fluid consists of soft spheres where the harmonic repulsion between two approaching particles starts when their distance is smaller than the sum of their radii. This model, originally proposed to describe wet foams[29], already finds experimental realizations in emulsions, soft colloids, and grains[30,31]. Although many results on its phase behaviors have been presented in theories and simulations over the last decades[13,16–19,32], its anomalous behaviors and the relevant scaling relation between thermodynamic and dynamic behavior are not known yet in detail. Furthermore, we should stress that a clear explanation of why the fluids with soft particles are different from 'simple' hard-sphere like fluids is still lacking until now. In order to address this point, we carry out molecular dynamics(MD) simulations in this study to investigate the structural and dynamical anomalies, as well as to analyze the entropic scaling for the system. We show that the soft particles behave like effective hard spheres only at sufficiently low temperatures and densities so as to make the Rosenfeld entropic scaling hold true. Especially the core-softened fluid exhibits an unusual configuration as the temperature is increased to high enough, i.e, the behavior of the system is like a weakly correlated mean-field fluid. Due to such a weakly correlated mean-field behavior, a scaling relation between the temperature scaled diffusion D_T and S_{ex} holds, and D_T is approximately inversely proportional to $-S_{ex}$ at least for soft particles interacted with harmonic repulsions. Therefore we believe that our original findings above may be valuable and contribute insightfully to the subject of anomalous behaviors in the fluids with ultrasoft interactions.

2 Model and Simulation Methodology

The soft particles are interacted by the harmonic repulsion, which is defined as

$$U(r_{ij}) = \begin{cases} \frac{\varepsilon}{2}(1 - r_{ij}/\sigma)^2, & r_{ij} < \sigma \\ 0, & r_{ij} \geq \sigma \end{cases} , \tag{3}$$

where r_{ij} is the pair distance between ith particle and jth particle. The parameter ε and σ governs the strength and maximum distance of the interaction, respectively. For the soft spherical particles, the maximum distance of the interaction σ is equal to their diameters.

To explore the dynamic properties of the systems, we perform MD simulations in canonical ensemble, i.e., the total number of particles N, the temperature T, and the volume of simulation cell V are kept constant. For convenience, the reduced units are used in the simulations. The basic units are chosen as follows: energy unit ε, length unit σ and the mass of particle m. The periodic boundary conditions are applied. The equation of motion is integrated using velocity Verlet algorithm[33,34] with the time step $\delta t = 0.01$, and the constant temperature is controlled via Berendsen thermostat[35].

The diffusion coefficient D can be calculated by fitting the long time average mean-squared displacement of the particles $\langle \delta r^2 \rangle$ according to the Einstein relation

$$6Dt = \langle \delta r^2 \rangle \, . \tag{4}$$

In order to investigate the relation between the anomalous dynamic behavior and the structural order, we need to calculate the value of the two-body excess entropy defined as

$$S_2 = -2\pi k_B \rho \int_0^\infty \{g(r)\ln[g(r)] - [g(r) - 1]\} r^2 dr \, , \tag{5}$$

where $g(r)$ is the pair correlation function(PCF) and ρ is the number density. For a completely uncorrelated system, $g(r) = 1$ and then $S_2 = 0$. For a system with a long-range order, spatial correlations persist over long distances and $-S_2$ becomes very large. Thus, S_2 can be taken as an indicator of structural order. This parameter yields information about the average relative spacing of the particles, i.e., it describes the tendency of particle pairs to adopt preferential separations.

Although the calculation of S_2 is very useful and the computation is easy, we also need to study the scaling relation between the diffusion D coefficient and the full excess entropy S_{ex}. For the systems with soft particles, the difference between S_{ex} and S_2 is large, especially when the density of the particles is high where three- and higher-body terms contribute significantly to the excess entropy. Below, we describe an approach for evaluating the full excess entropy[34]. Firstly the excess free energy F_{ex} is determined by

integrating the pressure $P(\rho)$ along an isotherm starting at low densities where the fluid behaves effectively as an ideal gas,

$$F_{ex} = N\int_0^{\infty} \frac{P(\rho) - k_B T\rho}{\rho^2} d\rho \ . \tag{6}$$

Then the excess entropy S_{ex} is obtained from the relation

$$S_{ex} = \frac{U - F_{ex}}{Nk_B T} \ , \tag{7}$$

where U is the internal potential energy of the system. In principle, thermodynamic integration(Eq.6) could also be done along the temperature to get F_{ex}, with the advantage that using five points(i.e., five simulations at different temperatures) already provides with rather accurate results[36,37]. Here the simulations are carried out for the isotherms $T = 0.01 - 0.1$ with the step of 0.01 and the isotherms $T = 0.2 - 1.0$ with step of 0.1. In making the thermodynamic integration, we used the simple trapezoidal rule which works rather accurately in this case. The integration is done over two density regions: from $\rho = 0.01$ to $\rho = 2.0$ with interval of $d\rho = 0.01$ and from $\rho = 2.0$ to $\rho = 10.0$ with interval of $d\rho = 0.04$, to ensure that the accuracy of the thermodynamic integration in both of the density regions is satisfactory.

3 Results and Discussion

According to the phase diagram constructed via thermodynamic integration[17], the maximum melting temperature of the system is $T_c \approx 6.35 \times 10^{-3}$. We perform all the simulations above the melting temperature to assure that the system is always in a fluid state. The number of particles is chosen as $N = 1000$, and the temperature is set from $T = 0.01$ to $T = 1.0$. Each simulation in NVT ensemble is carried out separately. For a typical simulation, the particles are put in the cubic box randomly and their velocities satisfy the Maxwell-Boltzmann distribution. After the system is relaxed to get an equilibrium, another run is done to calculate the average values of some parameters needed. The equilibration run is 10^5 time steps and the production run is 10^6 time steps for the accuracy.

Firstly, we investigate the dependence of self-diffusivity on density along a set of isotherms(see Fig.1), to study the dynamic behavior of the fluid. The diffusion coefficient, which decreases monotonically with increasing the density in normal liquids, shows a clear nonmonotonic behavior at low temperature. Compressing the low-density fluid initially decreases D, but the compression can eventually lead to an anomalous increase in D at sufficiently high density. The density $\rho \approx 2.0$ at which the minimum in D occurs as a boundary between the regions of normal and anomalous dynamic behavior can be seen in the top panel of Fig.1. Such dynamical anomalies have also been observed in other fluids with soft particles[4–6,38]. When the temperature is increased to high enough, the diffusion coefficient becomes to decay with increasing the

density and to come to an almost constant value finally(see the bottom panel of Fig.1), indicating that the dynamical anomaly disappears.

As is already mentioned, the quantity S_2 is the two-body contribution to the excess entropy and effectively characterizes the degree of structural order present in the fluid. It can be conveniently computed and analyzed given its straightforward connection to PCF(see Eq.5). Fig.2 displays the density dependence of S_2 calculated from MD along a series of isotherms in a density range up to $\rho = 10.0$. Like the diffusion coefficient, the two-body excess entropy S_2 has a minimum at low temperatures but it becomes a monotonically decreasing function of the density when increasing the temperature to high enough. Compared with the case of dynamical anomaly, the temperature where the region of structural anomaly disappears seems to be higher. Moreover, the curve obtained at $T = 0.01$(lowest temperature) not only goes through a minimum around $\rho = 2$, but then through a maximum around $\rho = 5.5$. This behavior suggests the presence of a second minimum above $\rho = 10$, so one may assume to get back the same large-ρ behavior as at all the other temperatures studied.

The quantity S_2 is connected with PCF, so the structural order is reflected by the formation of distinct first, second, and more distant coordination shells in $g(r)$. In Fig.3, the PCF curves for several density ranges at $T = 0.01$ are shown. Compression of the fluid initially leads to an increased height of the first peak in PCF, but further compression after a maximum makes the height of the first peak in PCF decrease. This investigation is in accord with the inspection of S_2 in Fig.2. Moreover, we should mention here that such a result is also consistent with the theoretical calculation of the system's structural anomaly via hypernetted chain approximation of liquid state theory, in which the theory predicts an anomalous(nonmonotonic) evolution of the intensity of the first peak when the density is increased at constant temperature[13]. In fact, the structural anomaly is physically a direct consequence of particle softness, which can be attributed to a competition between the energy and the entropy. At sufficiently low densities and low temperatures, the effective repulsive "core" of the soft potential is like the hard-sphere interaction to make the system behave as an effective hard-sphere fluid, so it can easily minimize energy by avoiding particle overlaps. In this regime, the structural order is increased with the increasing of the density as it does in a hard-sphere fluid. Further compression of the fluid make it harder and thus entropically less favorable to avoid particle overlaps because the repulsion between particles is too soft and the system must find more efficient ways to pack the particles. In other words, the system of soft particles only pays a finite potential-energy penalty for each overlap while avoiding overlaps carries a substantial entropic penalty, so the system tend to evolve toward a more uniform average structure at sufficiently high density. As a result, the structural order is decreased with the compression of the system in this regime.

It is useful to locate the boundaries of structural and dynamical anomalies as the curves of D and S_2 have been obtained. Fig.4 shows the estimated locations of the extrema of D and S_2 in $T-\rho$ plane. Obviously the

state points which exhibit the dynamical anomaly are a subset of those linked with the structural anomaly. Such a phenomenon qualitatively agrees with the finding reported by Krekelberg et al. concerning the anomalous behaviors of Gaussian-core(GC) fluid[4]. This qualitative agreement is not surprising because both GC and harmonic particles are belong to the core-softened particles with bounded potential. However, the densities of the boundaries of structural and dynamical anomalies in the fluid with harmonic particles are much larger than those in GC fluid, which is probably due to the different softness of particles between the two kinds of fluids. Compared with GC particles, the harmonic particles have harder repulsions so as to be able to "return" to hard spheres in a larger density.

Next, we consider the Rosenfeld scaling relation between the full excess entropy S_{ex} and the diffusion coefficient D for the fluid. In simple atomic fluids, S_2 is known to closely approximate S_{ex} at low to intermediate density[39,40]. However, the fluid with soft particles has a structural behavior which is very different from that of simple atomic fluids. In fact, there are often significant differences between S_2 and S_{ex} for the fluids with soft particles[6] due to the three- and higher-body contributions. Before the study of the Rosenfeld scaling relation between S_{ex} and the diffusivity, it would be useful to see the results of S_{ex}. Fig.5 presents the curves for S_{ex} as a function of the density ρ. Similar to the case of S_2, S_{ex} also shows a nonmonotonic density dependence along the isotherm at low temperatures, and it becomes a monotonically decreasing function of the density at high enough temperatures.

In Fig.6, the dependence of the Rosenfeld reduced diffusion D_R on the excess entropy along some isotherms is shown. Looking at the curves for low temperatures $T = 0.01 - 0.1$(see the top panel of Fig.6), we can divide these curves into two distinct regions with different slopes which are denoted as 1 and 2. The density increases in the right-to-left direction along a curve, i.e., region 2 has higher densities than region 1. Also seen from Fig.5, S_{ex} decreases with the increasing of density in the region of normal behavior; S_{ex} increases with the increasing of density in the region of anomalous behavior. With the increasing of temperature, region 2 become shorter and shorter. Already at $T = 0.2$, region 2 is negligibly small. As is seen from the plots at different temperatures and densities, the data of D_R versus $-S_{ex}$ apparently do not collapse onto a single curve. However, the plots of regions 1 at some low temperatures(up to $T = 0.05$) seem to collapse onto the same curve(see Fig.7). For comparison, Eq.1 and Eq.2 with parameters that fit the simulation data for a variety of model systems $A = 0.58$, $B = 0.78$(at high $-S_{ex}$) and $\alpha = 0.37$, $\beta = 2/3$(at low S_{ex}) are also shown in Fig.7. Apparently, the form of the relationship between the Rosenfeld reduced diffusion and the excess entropy is virtually the same, whether one considers the soft spheres with harmonic repulsions or a model system for hard-sphere and simple atomic fluid. Notice here that the volume fraction $\phi = \frac{\pi}{6}\rho\sigma^3 < 1$ in region 1. Therefore such observations can be explained in the following: the fluid act like hard-sphere and simple atomic fluids at rather low temperatures and densities where both structural and dynamical behaviors are normal, so as to make the Rosenfeld scaling relation valid for the

system. Furthermore, while the structural anomaly becomes less and less marked upon increasing the temperature resulting in the vanishing of region 2, the curves of D_R versus S_ex along different isotherms deviate significantly. In a word, the general scaling relations between D_R and S_{ex} does not work in the regions of structural anomaly and higher temperatures, which is just like the behaviors of other fluids with soft particles[4,6,14,15].

Another scaling formula for the systems with soft particles, which looks like the Rosenfeld one with density omitted, has been proposed. For instance, it was ever reported that the plots of $D_T = DT^{-1/2}$ versus S_{ex} approximately collapsed onto a single master curve in GC fluid[4]. Here we also plot the data of D_T versus S_{ex} for all the temperatures and densities studied, but do not see the plots collapse onto the same curve. Nevertheless, to further analyze the data, we find that the plots of D_T versus S_{ex} eventually collapse onto a single master curve when the temperature is increased to high enough($T \geq 0.2$, see Fig.8). It is still not known exactly why this alternative scaling holds for the core-softened fluids at present. Here we show that the fluid exhibits an unusual configuration. In the top panel of Fig.9, the PCF curves for some densities at rather high temperature $T = 0.5$ are displayed. It can be seen that there are fairly a few particles overlapped with each other, and that the particles become uncorrelated for long range($r > 1.0$) as $g(r)$ approaches unity. Next, we may consider the number of particles whose centers are, on average, within a distance r_c from a given particle in the fluid. This number of particles n_c can be calculated by

$$n_c = 1 + 4\pi\rho \int_0^{r_c} g(r) r^2 dr \,. \tag{8}$$

In the bottom panel of Fig.9, the curves of quantity $4\pi g(r)r^2$ within the distance $r = 1.0$ for several densities along $T = 0.5$ are shown. There is little deviation between the curves of different densities, which suggests that n_c is nearly a linear function of ρ and the particles are distributed almost uniformly. Therefore the system behaves as a weakly correlated mean-field fluid looking like an ideal gas. However, such a mean-field fluid is somewhat different from the usual ideal gases. With the increasing of temperature, the particles can easily penetrate each other because the thermal energy become more and more significant and may eventually dominate over the bounded potential. Actually, the system can be considered as a fluid consisting of most particles distributed uniformly which act as ideal gas and a few small clusters which are separated from each other. The self-diffusion coefficient is dominated by 'jumps' of particles in between clusters. According to Eq.8, one can expect that the average number of particles in each cluster(especially the particles sitting on top of each other) also linearly increases with the increasing of the macroscopic density ρ, indicating that the local density inside the clusters will not be affected strongly by the macroscopic density. In other words, even the average number of particles per cluster increases, the typical spacing between clusters remains constant. Hence the density does not influences the single-particle dynamics, making the density falls out of the scaling relation between the excess entropy and the diffusion coefficient.

For a further study of the scaling relation between D_T and S_{ex}, we have fitted the data of D_T versus $-S_{ex}$ in the regime of mean-field fluid behavior. We find that the temperature scaled diffusivity D_T is almost inversely proportional to $-S_{ex}$(see the dashed line in Fig.8), and the fitting formula can be given by

$$D_T \approx -0.22/S_{ex} \, . \tag{9}$$

At the moment, such a scaling formula between D_T and S_{ex} is only proved to be valid in the fluid with harmonically repulsive particles. And whether this kind of scaling formula can also be used in other fluids of bounded interaction needs a confirmation. Nevertheless we can at least say that the alternative scaling relation(D_T versus S_{ex}) holds seems to be relevant to the mean-field fluid behavior of the system. For instance, the system of Hertzian spheres is expected to exhibit a mean-field behaviors and to have a scaling relation similar to Eq.9 at high enough temperatures as Hertzian potential only has a rather minor modification in the exponent(from 2 to 2.5). To investigate the characteristics of the weakly correlated mean-field fluid, we have studied the compressibility factor $Z = \beta P/\rho$ and the excess free energy per particle F_{ex}/N in the regime where the alternative scaling relation D_T versus S_{ex} appears to hold. As can be seen in Fig.10, both the compressibility factor Z and the excess free energy per particle F_{ex}/N are approximately linear functions of the density ρ. This is rather like the equation of state reported in GC fluid[41]. Indeed the plots of D_T versus S_{ex} collapse onto a single master curve for all of the densities and temperatures studied in GC fluid[4], which is probably due to the fact that GC fluid exhibits such a mean-filed fluid behavior over a surprisingly wide range of densities and temperatures[41,42]. And the different regime of mean-filed behavior between harmonic spheres and GC fluid is possibly caused by the harshness of the potential, i.e, the GC interaction is softer.

It is also interesting to study the dependence of the Rosenfeld reduced diffusion D_R on the two-body excess entropy S_2. Previous researches on some other kinds of fluids with bounded potential, e.g Hertzian spheres and GC fluid, have shown that the plots of the Rosenfeld self-diffusivity D_R versus S_2 fall on the same master curve, despite the anomalous dependency of D and S_2 upon ρ. Here we have studied the scaling relations between D_R and S_2 for the system with harmonic spheres. In Fig.11, we show the curves of the Rosenfeld reduced diffusion D_R on the two-body excess entropy S_2 along different isochors for convenient comparison with previous results of other systems with soft particles. Apparently all of the plots at different densities approximately fall on the same master curve too, like the behaviors of other core-softened fluids[4,6]. Until now, such scaling relation has been shown to hold for several systems with soft particles, so it can be possibly expected to describe the behaviors of all the fluids with bounded potential. Nevertheless, further more studies in different systems need to be done to explore the issue whether this scaling relation between D_R and S_2 is generally valid in the fluids with bounded potential.

4 Conclusion

We present a detailed study on the behaviors of the fluid with harmonic repulsions via molecular dynamics simulation. Like the other systems with core-softened particles, the fluid exhibits both structural and dynamical anomalies especially at low temperatures, i.e, the dependence of the self-diffusivity D, the two-body excess entropy S_2 and the full excess entropy S_{ex} on the density ρ, is nonmonotonic. The Rosenfeld entropy scaling(D_R versus S_{ex}) to the system only holds true in the region of normal behaviors at sufficiently low temperature($T \leq 0.05$), where the soft particles may tend to avoid overlaps and behave like hard spheres or simple atomic particles. Furthermore, the Rosenfeld scaled diffusion D_R follows a scaling relation with the two-body excess entropy S_2 that is the same as what has been observed in other fluids with bounded potential. Such a coincidence is possibly general to the systems of bounded potential, but the conformation needs more careful studies in different systems. When the temperature is increase to high enough, the plots of the temperature scaled diffusion D_T versus S_{ex} collapse onto the same curve(D_T is inversely proportional to S_{ex} at least for this fluid with harmonic spheres), which is relevant to the fact that the system act as a weakly correlated mean-field fluid. We should mention here that the findings in this paper, especially the structural characteristic that distinguishes the different dynamical regimes, are not only limited to the fluid with harmonically repulsive particles. For instance, there is only a rather minor modification in the exponent for Hertzian model so that most of the findings can definitely apply to Hertzian spheres. Besides GC fluid, other core-softened fluids(e.g, Ref.[20]) that exhibit weakly correlated mean-filed behavior should also have a scaling relation between D_T and S_{ex}, which make the further studies desired.

5 Acknowledgements

This work is supported by Grants Nos. 11172302, 20903112, 10972217 and 11032011 from the National Natural Science Foundation of China.

References

1 P. G. Debenedetti, *Metastable Liquids: Concepts and Principles*, Princeton University Press, Princeton, 1996.

2 E. A. Jagla, *J. Chem. Phys.*, 1999, **111**, 8980–8986.

3 F. Saija, S. Prestipino and G. Malescio, *Phys. Rev. E*, 2009, **80**, 031502.

4 W. P. Krekelberg, T. Kumar, J. Mittal, J. R. Errington and T. M. Truskett, *Phys. Rev. E*, 2009, **79**, 031203.

5 J. C. Pàmies, A. Cacciuto and D. Frenkel, *J. Chem. Phys.*, 2009, **131**, 044514.

6 Y. D. Fomin, V. N. Ryzhov and N. V. Gribova, *Phys. Rev. E*, 2010, **81**, 061201.

7 E. Lascaris, G. Malescio, S. V. Buldyrev and H. E. Stanley, *Phys. Rev. E*, 2010, **81**, 031201.

8 E. Salcedo, A. B. de Oliveira, N. M. Barraz, C. Chakravarty and M. C. Barbosa, *J. Chem. Phys.*, 2011, **135**, 044517.

9 Y. D. Fomin, E. N. Tsiok and V. N. Ryzhov, *Phys. Rev. E*, 2013, **87**, 042122.

10 D. Nayar and C. Chakravarty, *Phys. Chem. Chem. Phys.*, 2013, **15**, 14162–14177.

11 G. Malescio, *J. Phys.: Condens. Matter*, 2007, **19**, 073101.

12 C. N. Likos, *Phys. Rep.*, 2001, **348**, 267–439.

13 H. Jacquin and L. Berthier, *Soft Matter*, 2010, **6**, 2970–2974.

14 M. J. Pond, J. R. Errington and T. M. Truskett, *J. Chem. Phys.*, 2011, **134**, 081101.

15 M. J. Pond, J. R. Errington and T. M. Truskett, *Soft Matter*, 2011, **7**, 9859–9862.

16 L. Berthier, E. Flenner, H. Jacquin and G. Szamel, *Phys. Rev. E*, 2010, **81**, 031505.

17 Y. L. Zhu and Z. Y. Lu, *J. Chem. Phys.*, 2011, **134**, 044903.

18 L. Berthier, H. Jacquin and F. Zamponi, *Phys. Rev. E*, 2011, **84**, 051103.

19 L. Berthier and T. A. Witten, *Europhys. Lett.*, 2009, **86**, 10001.

20 C. N. Likos, A. Lang, M. Watzlawek and H. Löwen, *Phys. Rev. E*, 2001, **63**, 031206.

21 S. Prestipino, F. Saija and P. V. Giaquinta, *Phys. Rev. E*, 2005, **71**, 050102(R).

22 N. Xu, T. K. Haxton, A. J. Liu and S. R. Nagel, *Phys. Rev. Lett.*, 2009, **103**, 245701.

23 M. van Hecke, *J. Phys.: Condens. Matter*, 2010, **22**, 033101.

24 A. Ikeda and K. Miyazaki, *Phys. Rev. Lett.*, 2011, **106**, 015701.

25 Y. Rosenfeld, *Phys. Rev. A*, 1977, **15**, 2545–2549.

26 Y. Rosenfeld, *J. Phys.: Condens. Matter*, 1999, **11**, 5415–5427.

27 J. Mittal, J. R. Errington and T. M. Truskett, *J. Chem. Phys.*, 2006, **125**, 076102.

28 J. Mittal, J. R. Errington and T. M. Truskett, *J. Phys. Chem. B*, 2007, **111**, 10054–10063.

29 D. J. Durian, *Phys. Rev. Lett.*, 1995, **75**, 4780–4783.

30 Z. X. Zhang, N. Xu, D. T. N. Chen, P. Yunker, A. M. Alsayed, K. B. Aptowicz, P. Habdas, A. J. Liu, S. R. Nagel and A. G. Yodh, *Nature*, 2009, **459**, 230–233.

31 J. Mattsson, H. M. Wyss, A. Fernandez-Nieves, K. Miyazaki, Z. B. Hu, D. R. Reichman and D. A. Weitz, *Nature*, 2009, **462**, 83–86.

32 B. Sun, Z. W. Sun, W. Z. Ouyang and S. H. Xu, *J. Chem. Phys.*, 2014, **140**, 134904.

33 M. P. Allen and D. J. Tildesley, *Computer Simulation of Liquids*, Clarendon Press, Oxford, 1987.

34 D. Frenkel and B. Smit, *Understanding Molecular Simulation: From Algorithms to Applications*, Academic Press, San Diego, 2nd edn., 2001.

35 H. J. C. Berendsen, J. P. M. Postma, W. F. Vangunsteren, A. Dinola and J. R. Haak, *J. Chem. Phys.*, 1984, **81**, 3684–3690.

36 M. Darvas, P. Jedlovszky and G. Jancsó, *J. Phys. Chem. B*, 2009, **113**, 7615–7620.

37 A. Idrissi, K. Polok, M. Barj, B. Marekha, M. Kiselev and P. Jedlovszky, *J. Phys. Chem. B*, 2013, **117**, 16157–16164.

38 W. P. Krekelberg, M. J. Pond, G. Goel, V. K. Shen, J. R. Errington and T. M. Truskett, *Phys. Rev. E*, 2009, **80**, 061205.

39 R. D. Mountain and H. J. Raveché, *J. Chem. Phys.*, 1971, **55**, 2250–2255.

40 A. Baranyai and D. J. Evans, *Phys. Rev. A*, 1989, **40**, 3817–3822.

41 A. A. Louis, P. G. Bolhuis and J. P. Hansen, *Phys. Rev. E*, 2000, **62**, 7961–7972.

42 A. Lang, C. N. Likos, M. Watzlawek and H. Löwen, *J. Phys.: Condens. Matter*, 2000, **12**, 5087–5108.

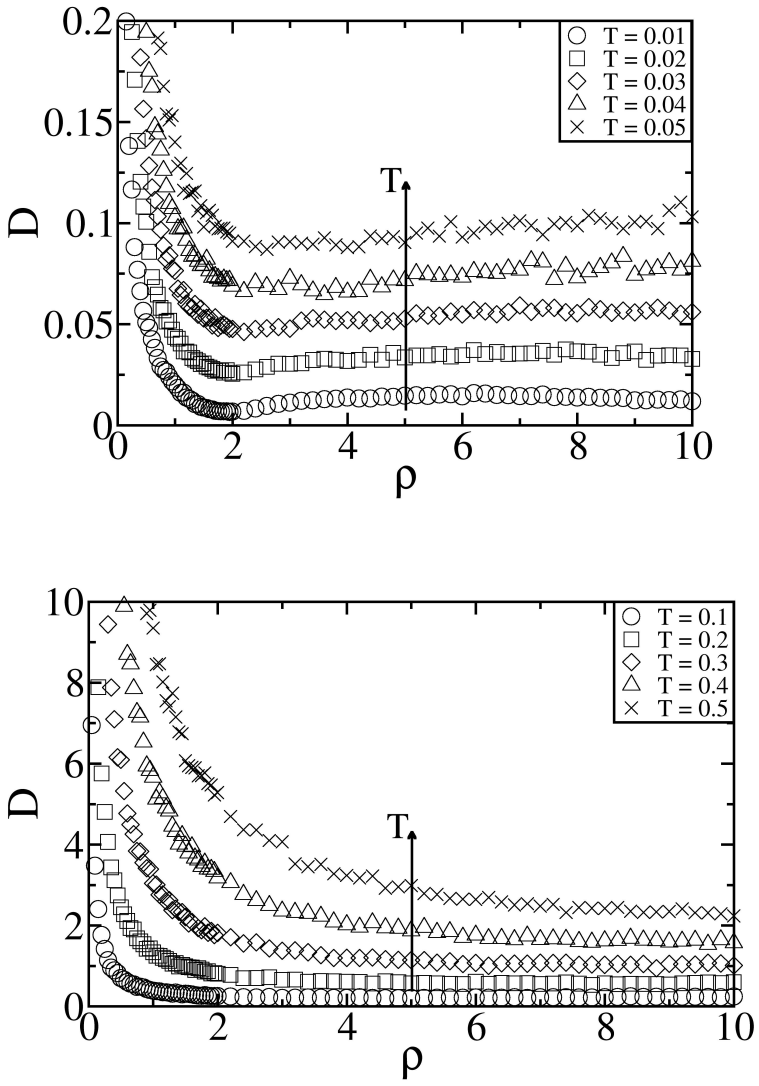

Fig. 1 The dependence of the diffusion coefficient D on the density ρ along a set of isotherms. Top: $T = 0.01, 0.02, 0.03, 0.04, 0.05$. Bottom: $T = 0.1, 0.2, 0.3, 0.4, 0.5$. The arrows indicate increasing the temperature T.

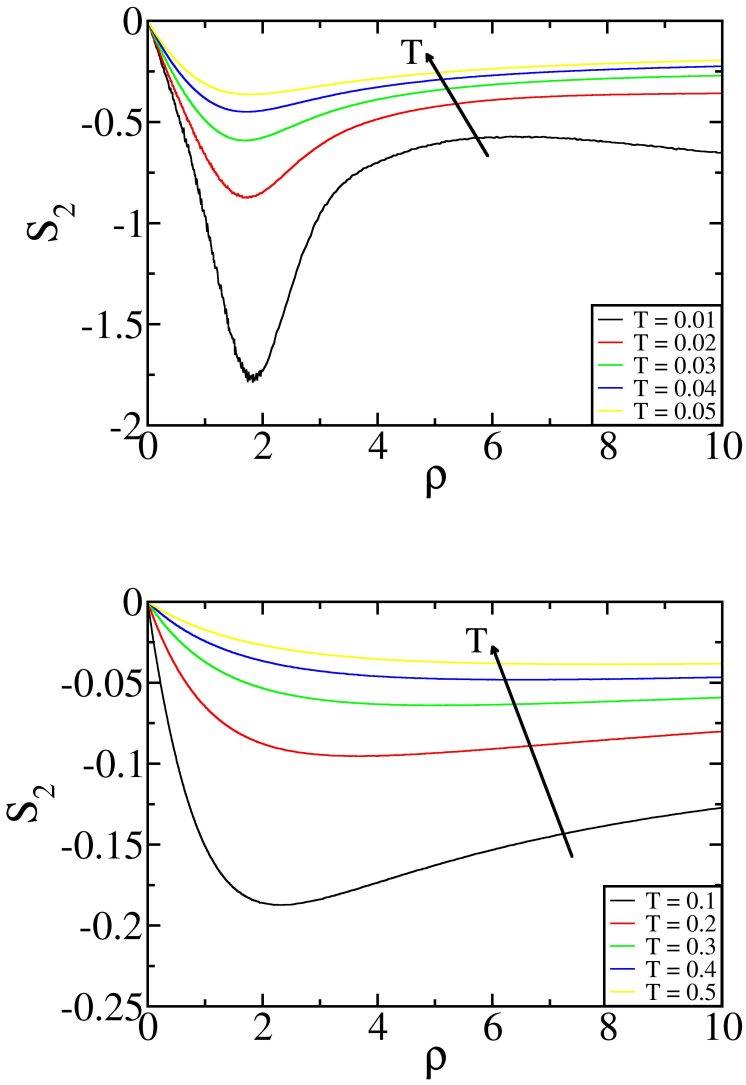

Fig. 2 The dependence of the two-body excess entropy S_2(structure order metric) on the density ρ along a set of isotherms. Top: $T = 0.01, 0.02, 0.03, 0.04, 0.05$. Bottom: $T = 0.1, 0.2, 0.3, 0.4, 0.5$. The arrows indicate increasing the temperature T.

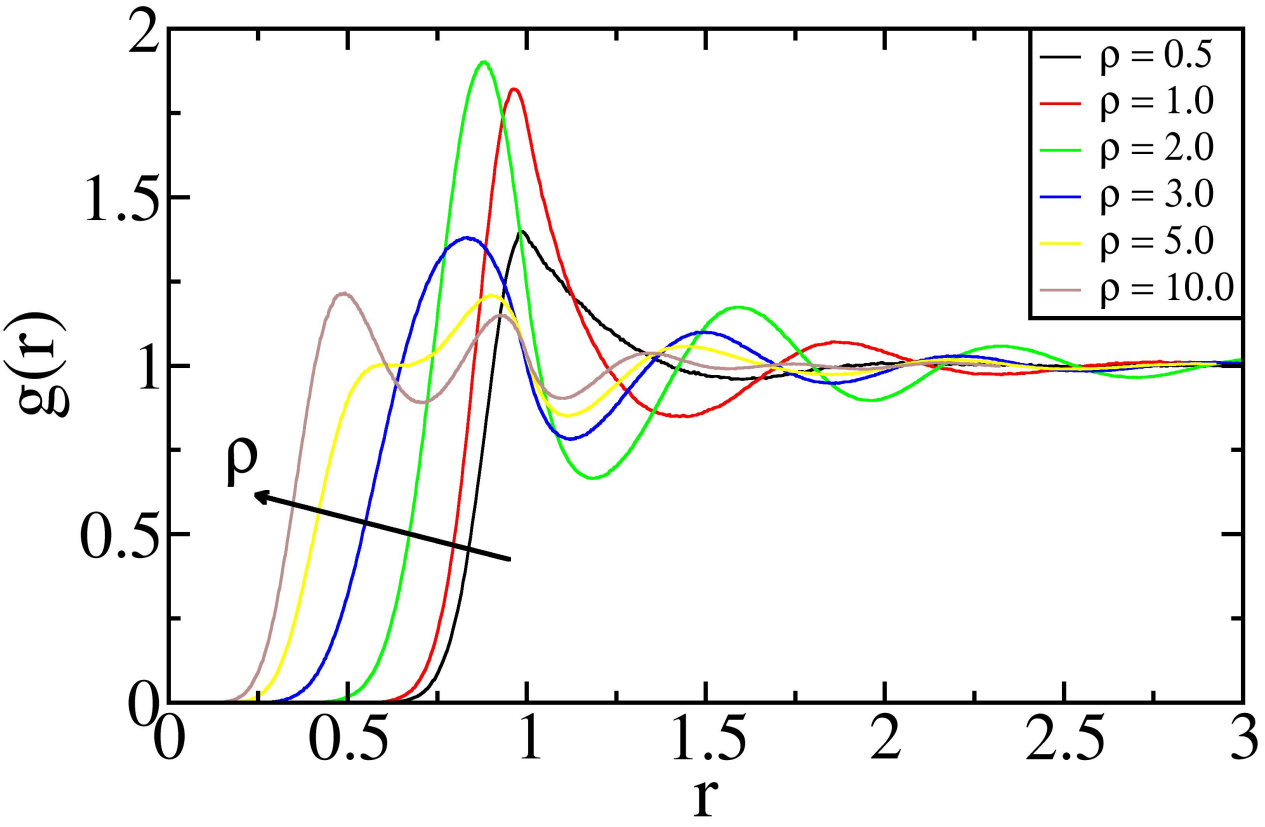

Fig. 3 Pair correlation function $g(r)$ for several densities along the isotherm $T = 0.01$. The arrow indicates increasing the density ρ. From right to left: $\rho = 0.5, 1.0, 2.0, 3.0, 5.0, 10.0$.

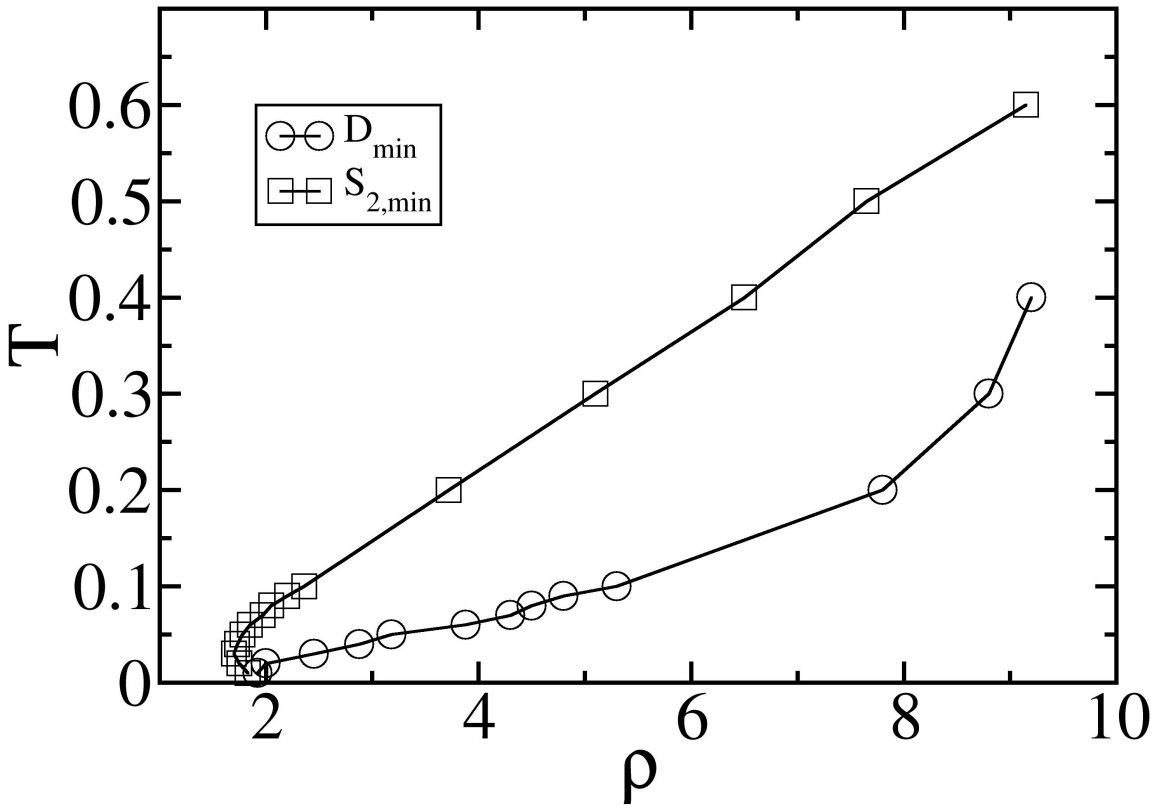

Fig. 4 Boundaries of the structural and dynamical anomalies in the $T-\rho$ plane, estimated from the data of simulations. Circle(Square) represents the density where $D(S_2)$ has a minimum at each temperature.

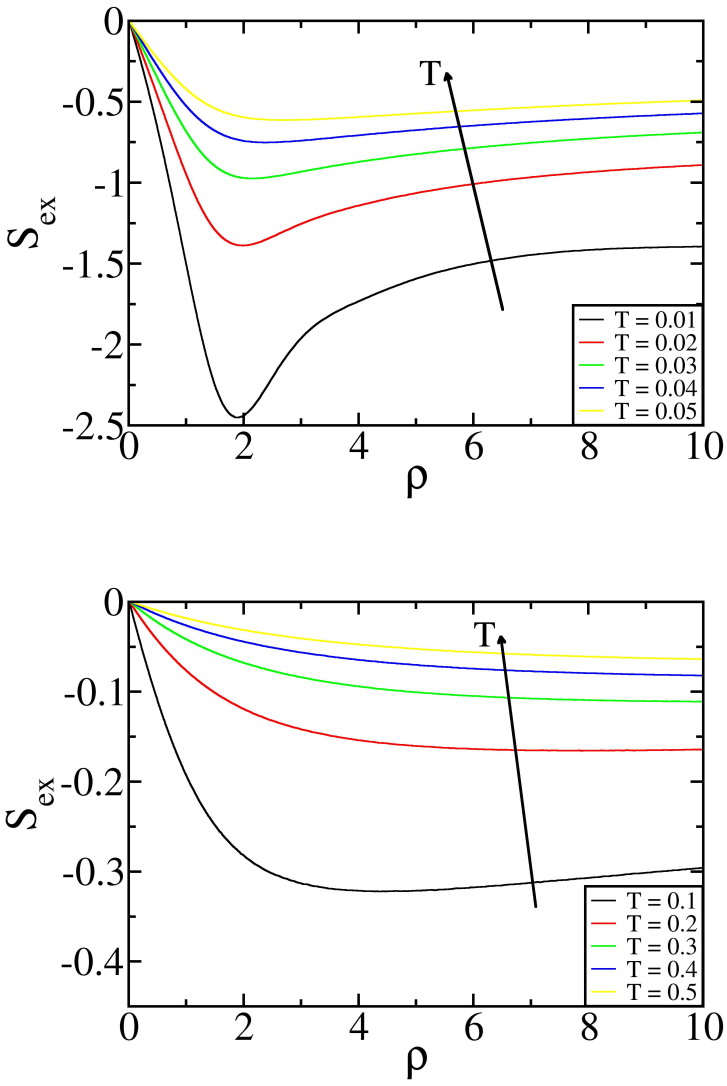

Fig. 5 The dependence of the excess entropy S_{ex} on the density ρ along a set of isotherms. Top: $T = 0.01, 0.02, 0.03, 0.04, 0.05$. Bottom: $T = 0.1, 0.2, 0.3, 0.4, 0.5$. The arrows indicate increasing the temperature T.

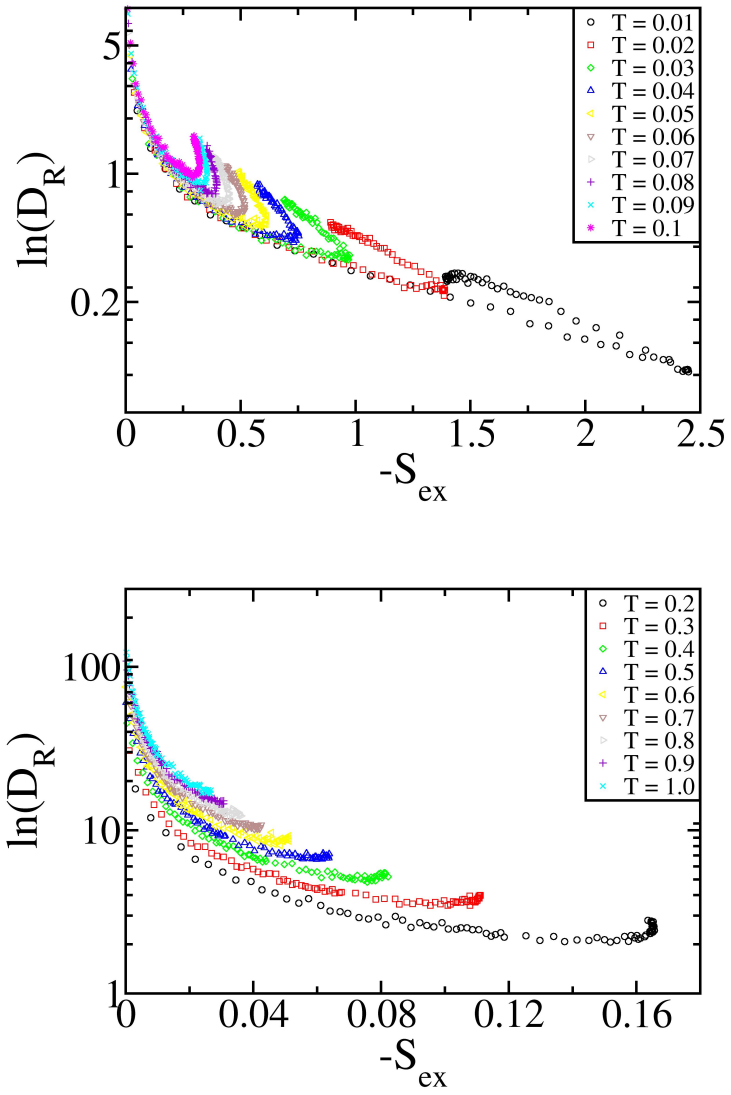

Fig. 6 The Rosenfeld scaled diffusivity $D_R = D\rho^{1/3}T^{-1/2}$ versus the excess entropy $-S_{ex}$ along a set of isotherms. Top: low-temperature behaviors from $T = 0.01$ to $T = 0.1$. Bottom: high-temperature behaviors from $T = 0.2$ to $T = 1.0$.

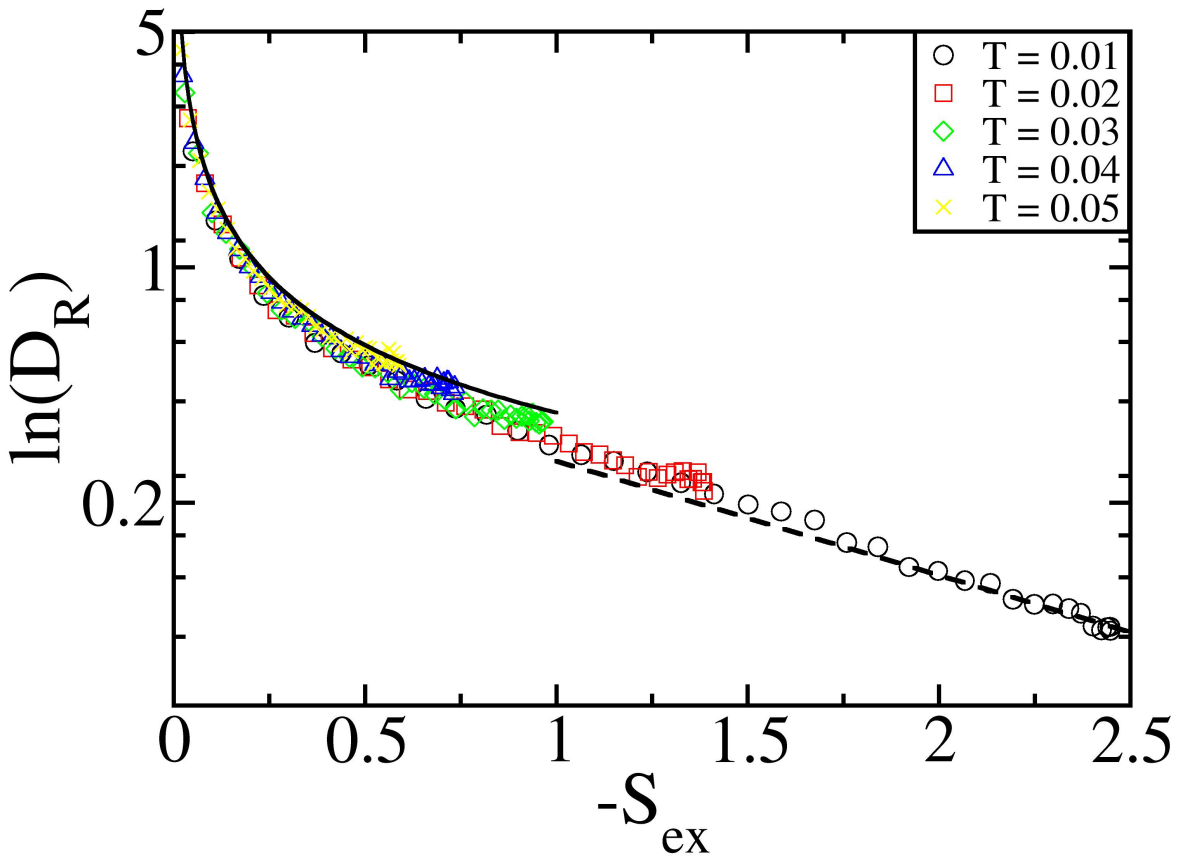

Fig. 7 The Rosenfeld scaled diffusivity D_R versus the excess entropy $-S_{ex}$ when the volume fraction $\phi < 1.0$ and the temperatures $T \leq 0.05$. The dashed line represents the empirical Rosenfeld scaling law $D_R = 0.58\exp(0.78S_{ex})$ and the solid line represents the low-density behavior expected as the power-law form $D_R = 0.37(-S_{ex})^{2/3}$.

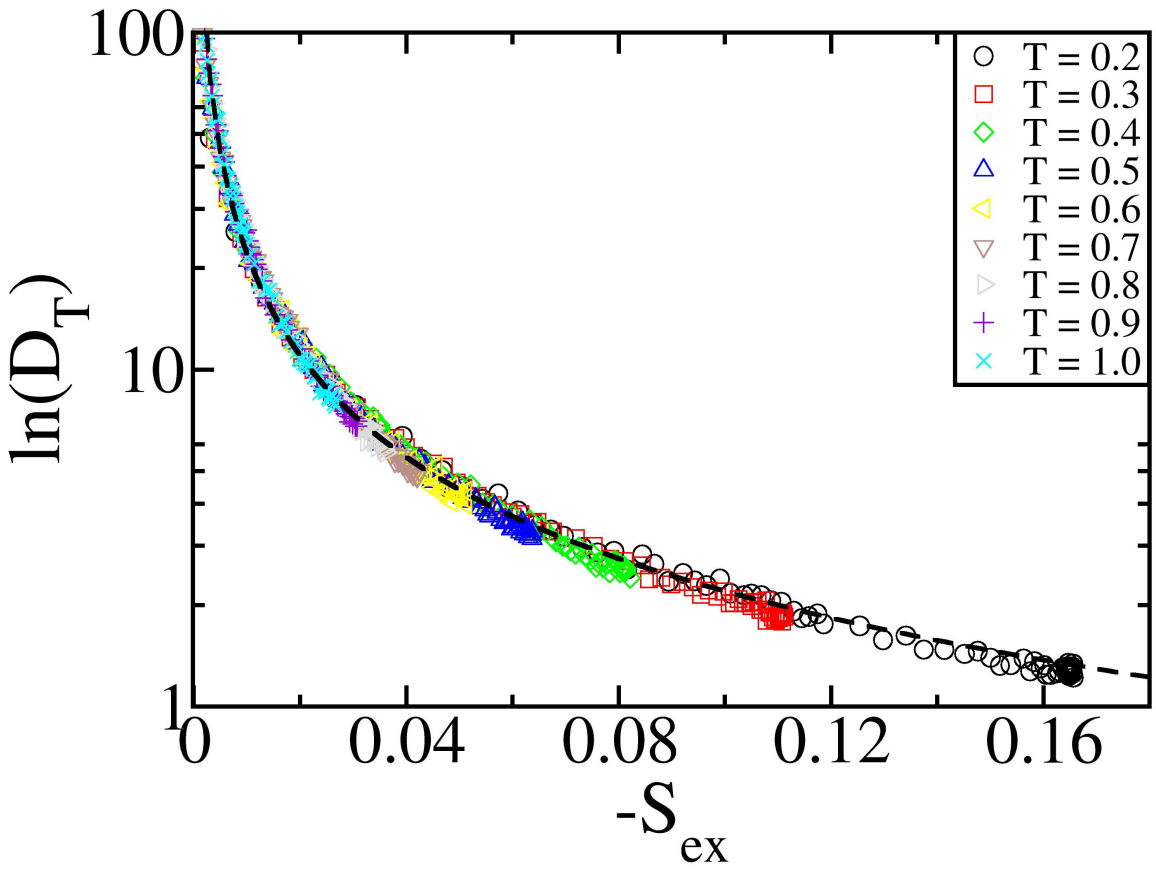

Fig. 8 The temperature scaled diffusivity $D_T = DT^{-1/2}$ versus $-S_{ex}$ along a set of isotherms from $T = 0.2$ to $T = 1.0$. The dashed line represents the curve of fitting function $D_T = -0.22/S_{ex}$.

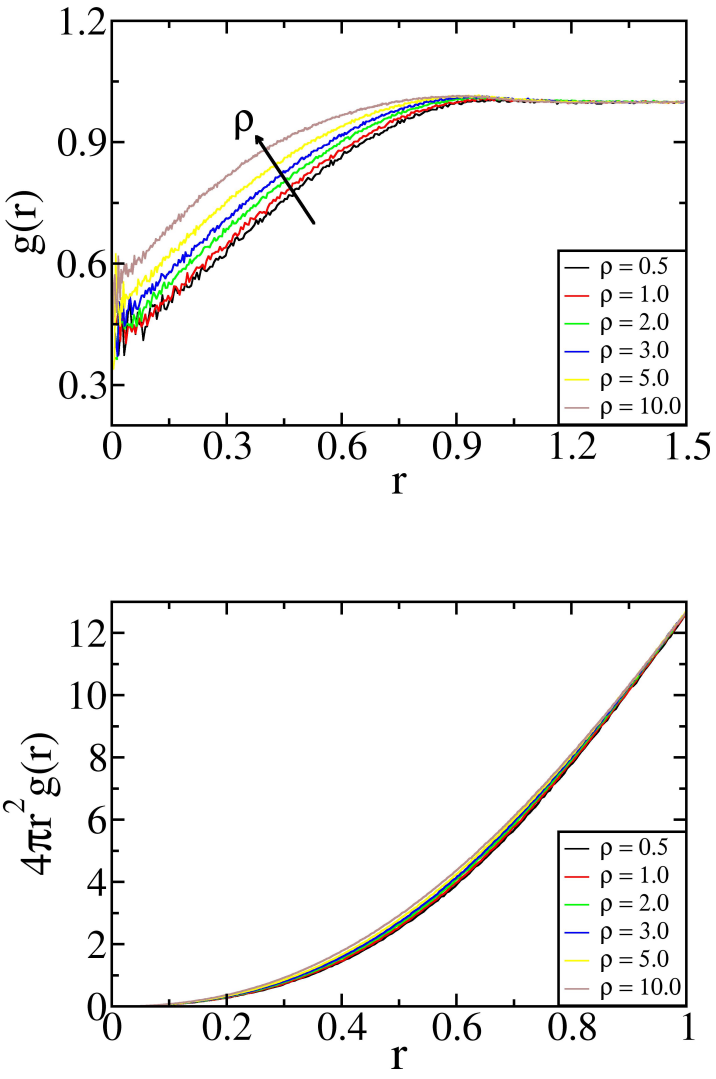

Fig. 9 Top: Pair correlation function $g(r)$ for several densities along the isotherm $T = 0.5$. The arrow indicates increasing ρ. Bottom: The quantity $4\pi r^2 g(r)$ within the distance $r_c = 1.0$ for several densities at $T = 0.5$.

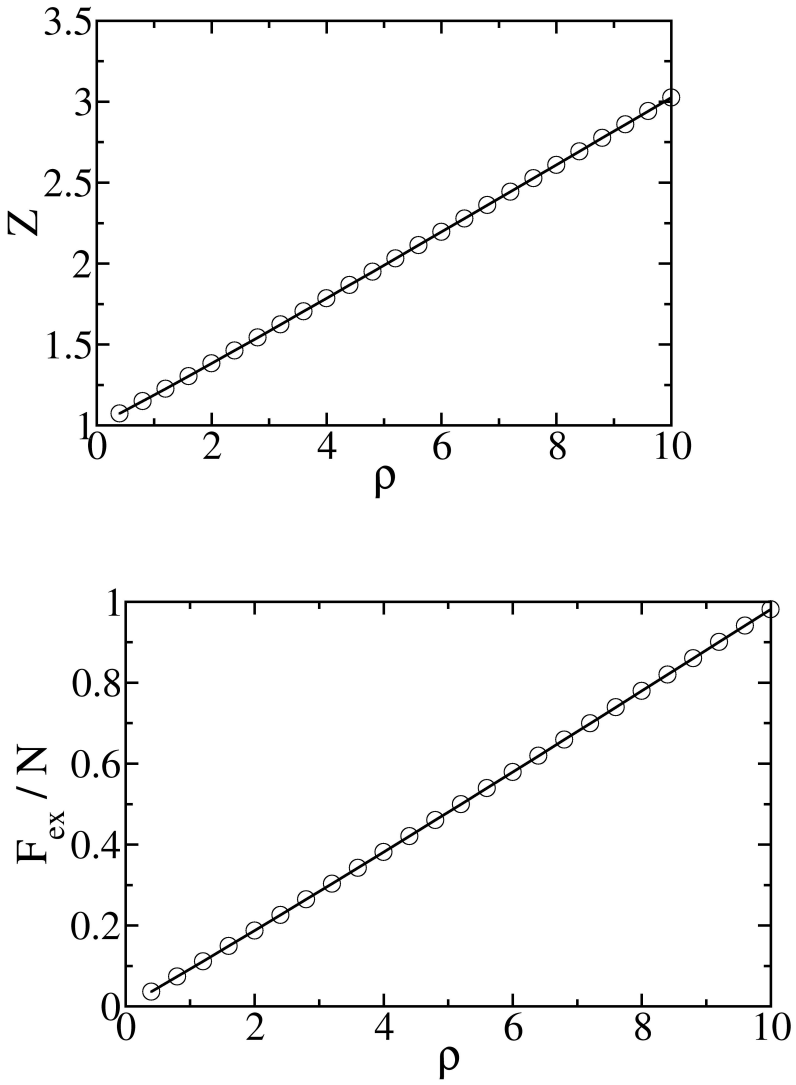

Fig. 10 Top: The dependence of the compressibility factor $Z = \beta P/\rho$ on the density ρ at $T = 0.5$. Bottom: The dependence of the excess free energy per particle F_{ex}/N on the density ρ at $T = 0.5$. Notice that the symbol sizes are larger than error bars.

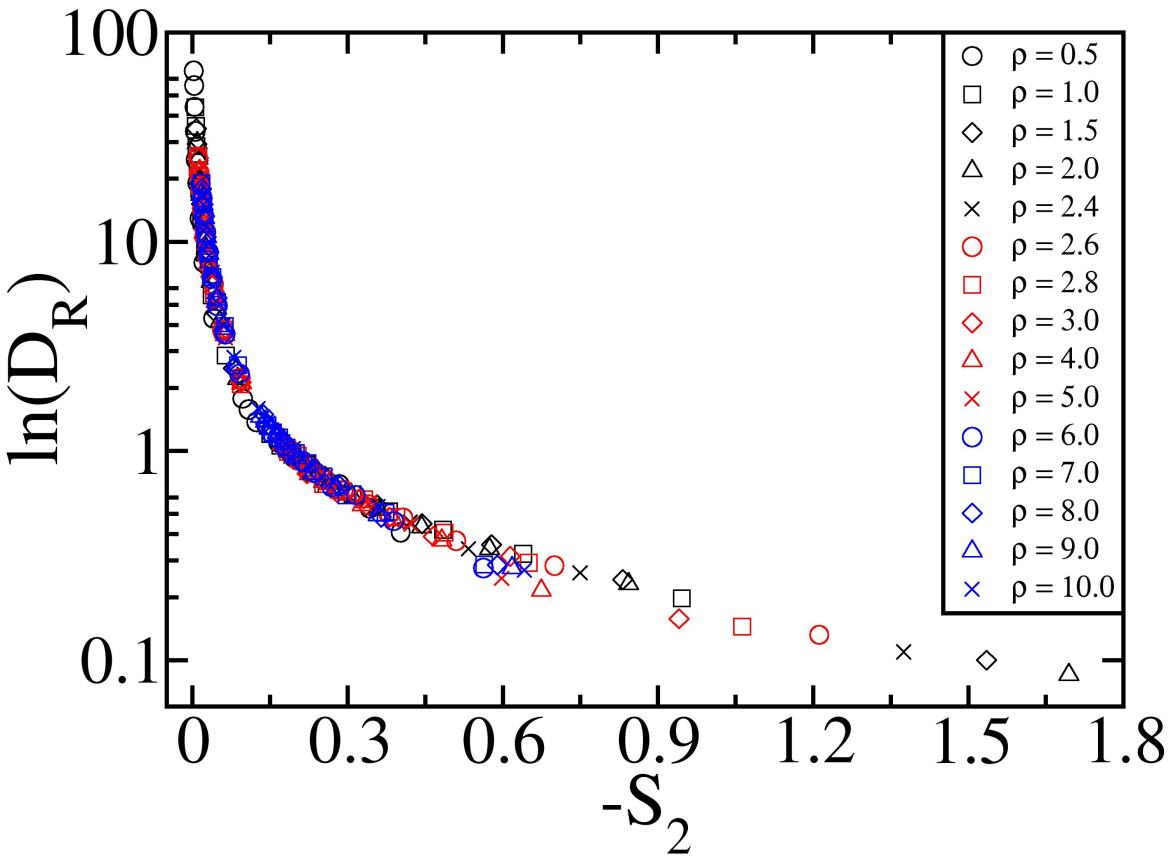

Fig. 11 The Rosenfeld scaled diffusivity D_R versus $-S_2$ along different isochors.